Electronic Supplementary Information (ESI)

Promoting photocatalytic H_2 evolution by tuning cation deficiency in La and Cr co-doped $SrTiO_3$

Jianing Hui,[a] Guan Zhang,*[ab] Chengsheng Ni[a] and John T. S. Irvine*[a]

[a] School of Chemistry, University of St Andrews, St Andrews KY16 9ST, UK.

[b] School of Civil and Environmental Engineering, Harbin Institute of Technology,Shenzhen, Shenzhen 518055, China.

E-mail: zhangguan@hit.edu.cn, jtsi@st-andrews.ac.uk

Experimental

Sample preparation

The La and Cr co-doped $SrTiO_3$ (LSCT) samples with different A-site cation deficiency were prepared via solid state method. For example, $La_{0.06}Sr_{0.94}Cr_{0.06}Ti_{0.94}O_3$, $La_{0.06}Sr_{0.91}Cr_{0.06}Ti_{0.94}O_{3-\delta}$, $La_{0.2}Sr_{0.7}Cr_{0.06}Ti_{0.94}O_{3-\delta}$, $La_{0.4}Sr_{0.4}Cr_{0.06}Ti_{0.94}O_{3-\delta}$ with A-site cation deficiency of 0%, 3%, 10% and 20 % were prepared and assigned as LSCT(0), LSCT(3), LSCT(10) and LSCT(20) according to the percentage of their cation deficiency, respectively. High purity raw materials (La_2O_3, $SrCO_3$ and TiO_2) were dried, weighed and mixed in acetone by corresponding ratios. Small amount of dispersant (KD1) was added into mixture to form suspension. An ultrasonic probe (Hielscher UP200S) was applied to break the agglomerates into fine powders. Stoichiometric quantity of $Cr(NO_3)_3 \cdot 9H_2O$ was dissolved in deionized water and added into suspension before evaporating excess acetone on hot plate (60 °C) with magnetic stirring. After this, the dry powder mixture was calcined at 1000 °C for 12 h. Then it was milled on a planetary ball mill (Fritsch pulverisette 7) at speed of 500 rpm for 2 h. The resulting powder was dried and pressed uniaxially to be dense pellets, and then fired at 1250° C for 16 h. The sintered pellets were crashed and ball milled at speed of

500 rpm for 2 h to be fine powder.

Characterization

The crystal structure and phase purity was confirmed with X-ray powder diffraction (XRD) on a PANalytical Empyrean Reflection Diffractometer (Cu Kα1 radiation). The obtained XRD patterns were analyzed with MDI Jade 6 software to see the crystal structure. And selected samples were refined using FullProf software. The microstructures of the samples were examined on a field emission scanning electron microscope (JEOL, JSM 6700) and transmission electron microscope (JEOL, JEM 2001). To compare the particle size of these powders, particle size was analyzed using a Malvern Instrument Mastersizer 2000 with a Hydro S sample dispersion unit. The specific surface areas (Brunauer-Emmett -Teller, BET) measurements were carried out on a Micrometrics TriStar II 3020 instrument. The surface elemental analysis of sample powders by X-ray photoelectron spectroscopy (XPS) was obtained using the Mg Kα line (1253.6 eV) as the excitation source. C*1s* peak at 284.6 eV was used as reference. UV-vis absorbance spectra were collected on an ultraviolet-visible spectrophotometer (JASCO-V550). The absorbance was transformed by the Kubelka-Munk method to calculate band-gap energy. The flat-band potentials were measured according Mott-Schottky method in a home-made cell with a three electrodes system. The dense sample pellet (D= 1.2 cm) coated with a thin layer of Ag paste for current collection was used as working electrode. 0.4 M Na_2SO_4 aqueous solution was used as the electrolyte. The impedance between -0.4 V and 1.0 V *vs*. Ag/AgCl reference was carried on a HF frequency response analyzer (SI 1255, Solartron) in the frequency range between 100 kHz and 0.1 Hz with a sine wave perturbation of 20 mV. Metal oxygen bonding stretching vibrations was detected by a fourier transform infrared spectrophotometer(IRAffinity-1S, SHIMADZU).

Photocatalytic H_2 production

The fine sintered powder (0.5 g) was infiltrated with 5 mL 2g/L H_2PtCl_6 aqueous solution and dried on hot plate at 90 ^{o}C with magnetic stirring. The powder was further

heated at 180 °C for 2 h to decompose H_2PtCl_6 into Pt or PtO_x. The ratio of loaded Pt or PtO_x species on LSCT sample was about 1.0 wt%. H_2 evolution experiments were carried out with 100 mg sample powders suspended in 100 ml 5 M NaOH solution filled with 10 vol% methanol. The suspension was sealed in a home-made photoreactor with headspace of ca. 0.55 L. Visible light irradiation was generated by a 250 W iron-doped metal halide Ultraviolet-Visible lamp with an Ultraviolet cut-off filter (≥ 420 nm; Borosilicate Coated Glass HM07, UQG (optic), Cambridge UK). Before photoirradiation, the sealed photoreactor was purged with Ar for 1 h to remove the O_2 and N_2 in air. The evolved H_2 in the head-space of photoreactor under irradiation were examined using an online gas chromatograph (Agilent 3000 Micro Gas chromatograph). During 6 h irradiation, the temperature of photoreactor increased from ~ 25 °C to ~ 40 °C. At least two tests were repeated for each sample. The pellet electrodes were also employed to test the photocurrent under visible light in a 5 M NaOH solution with a potential bias of +0.4 V vs. Ag/AgCl. Visible light irradiation was generated by a 250 W iron-doped metal halide Ultraviolet-Visible lamp with an Ultraviolet cut-off filter (≥ 420 nm).

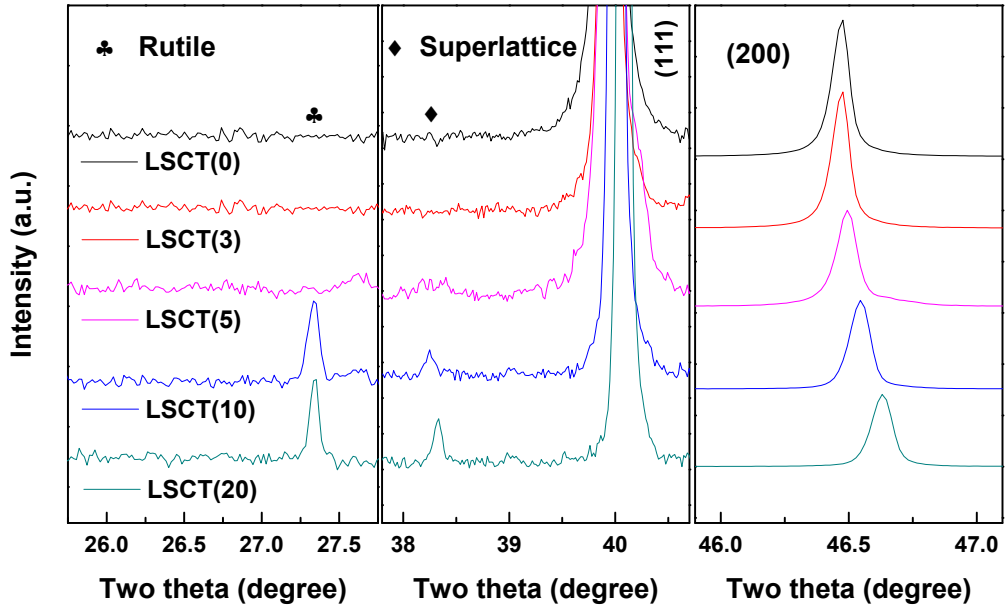

Fig. S1 X-ray diffraction patterns: Rutile peak in highly deficient samples (left); Superlattice peak from out-of-phase octahedral tilting in highly deficient samples (middle); (200) peak shifts as A site deficiency in LSCT samples (right).

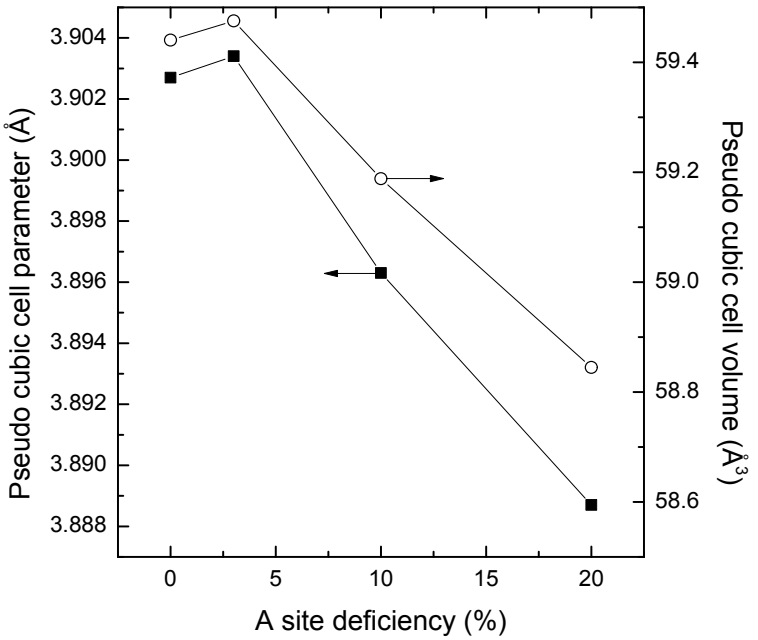

Fig. S2 The trends between the Unit cell parameters and the A-site cation deficiency for LSCT samples.

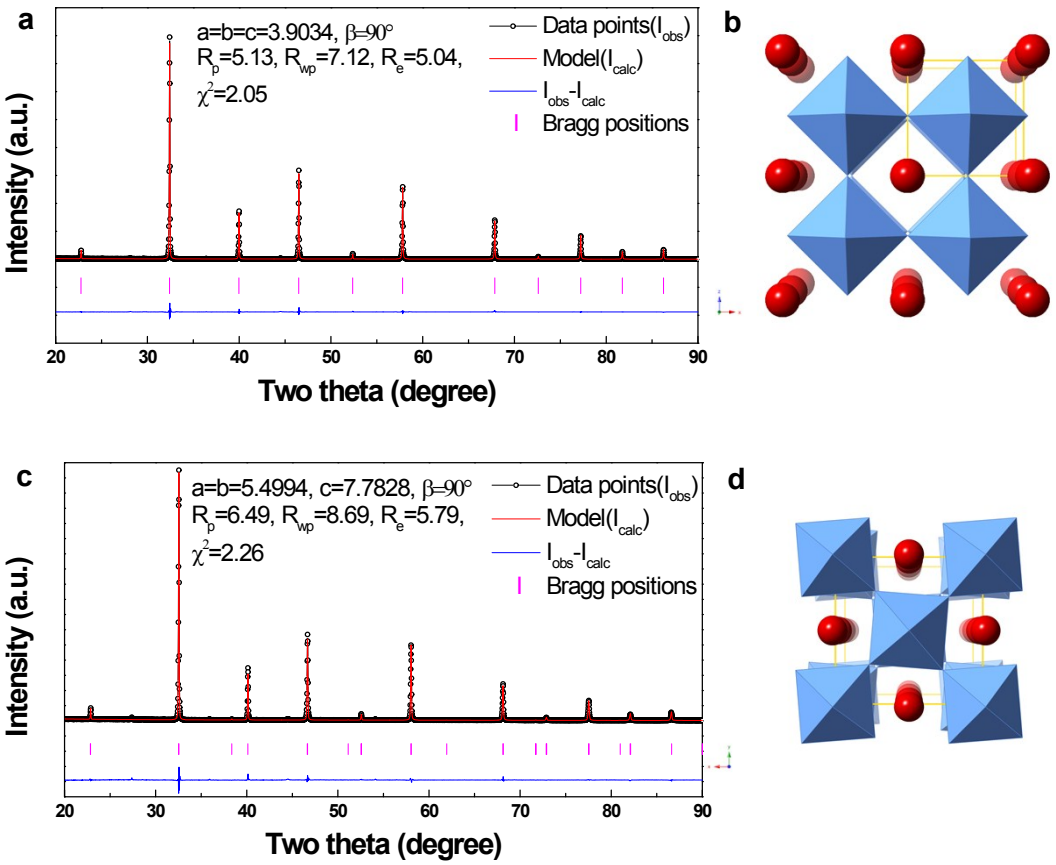

Fig. S3 Rietveld refinement results of a: LSCT(3) and c: LSCT(20); their crystal structure illustrations b: LSCT(3), d: LSCT(20).

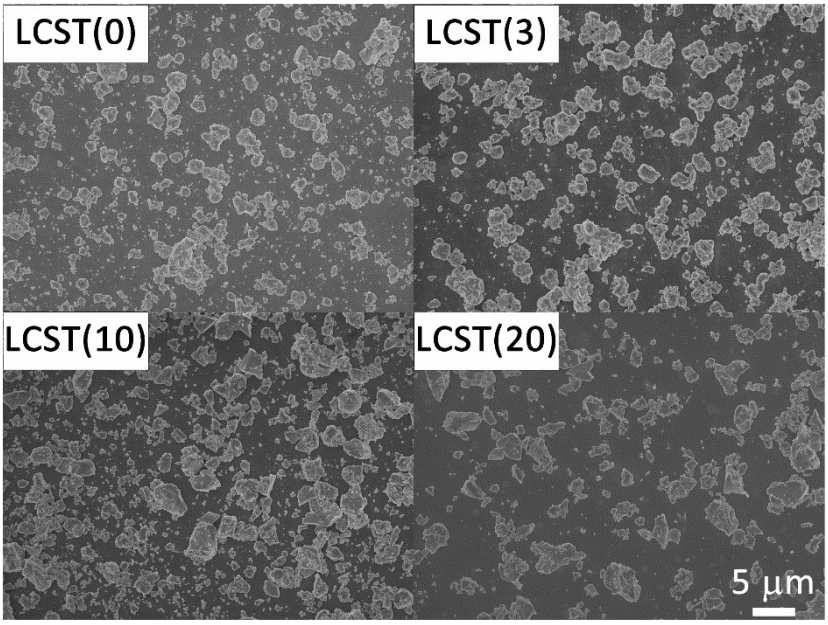

Fig. S4 SEM images of ball milled LSCT samples.

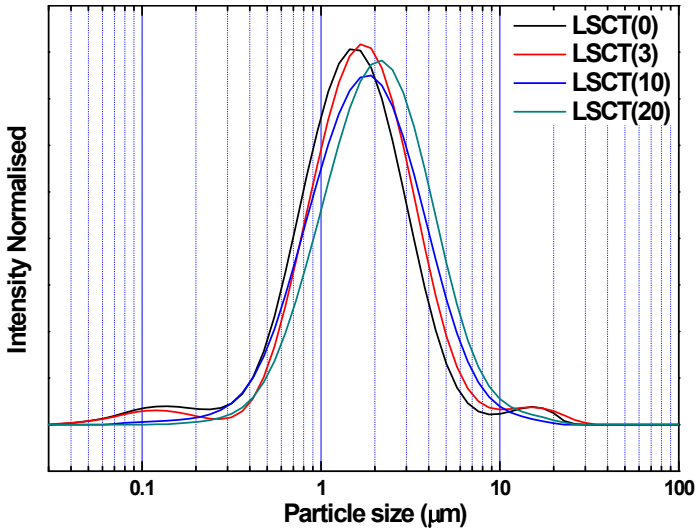

Fig. S5 Particle size distribution of ball-milled LSCT samples.

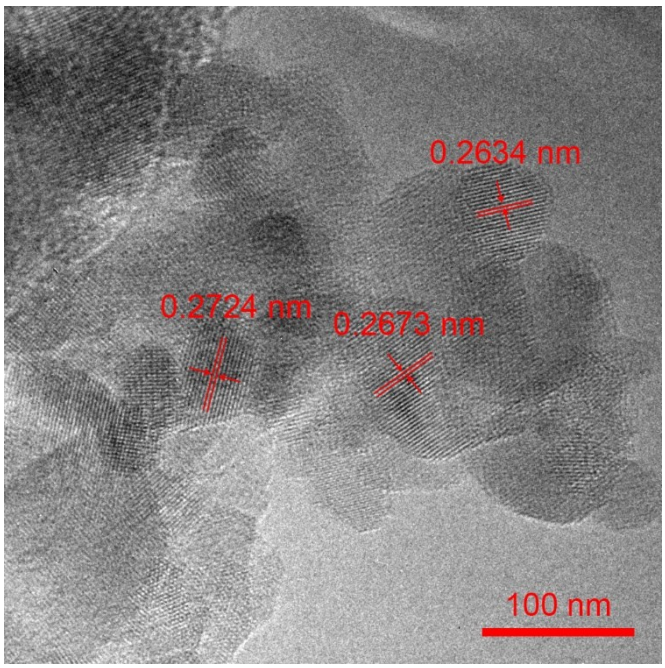

Fig. S6 High resolution TEM image of LSCT(3) sample.

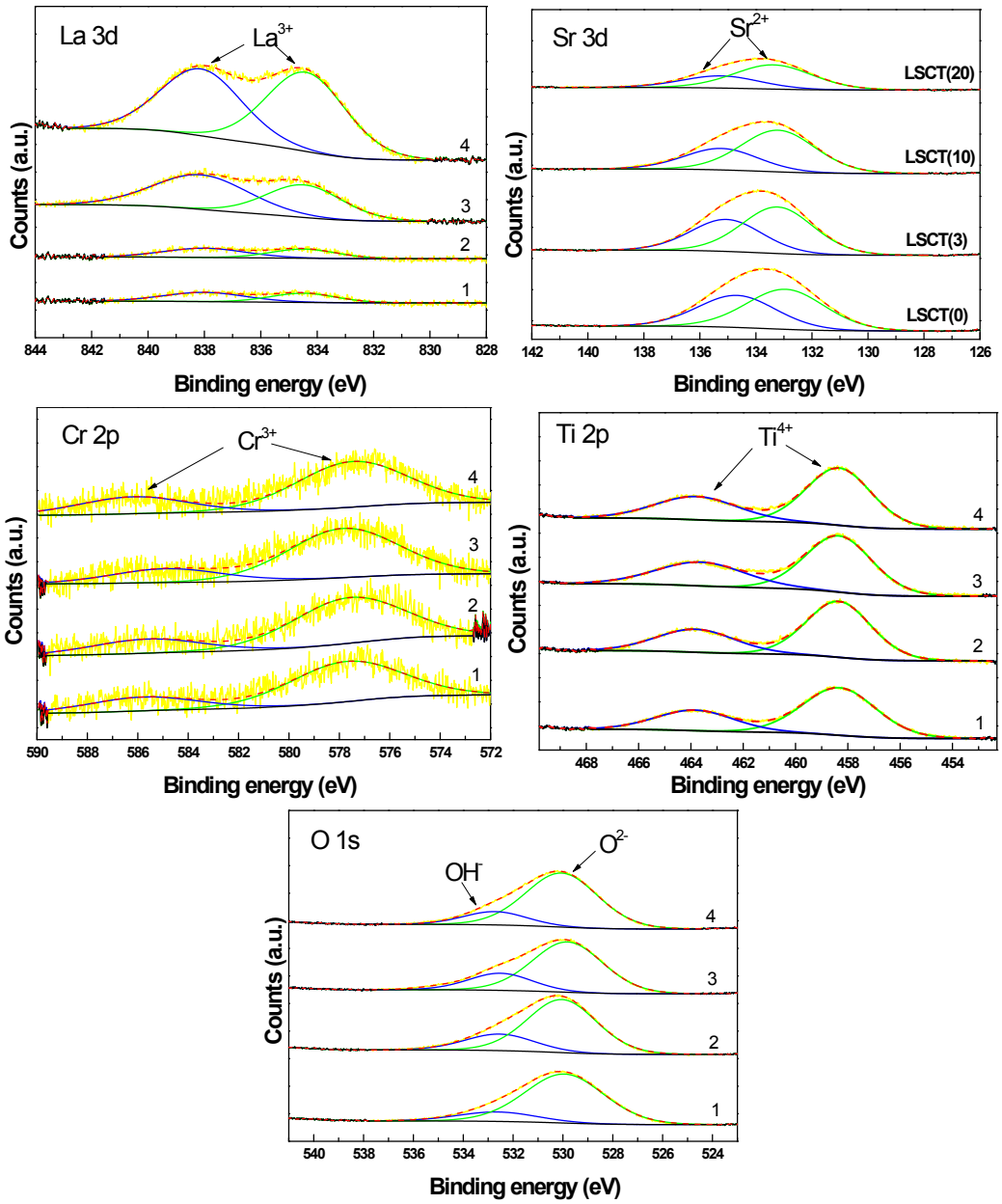

Fig. S7 La *3d*, Sr *3d*, Cr *2p*, Ti *2p* and O *1s* XPS spectra of LSCT samples.

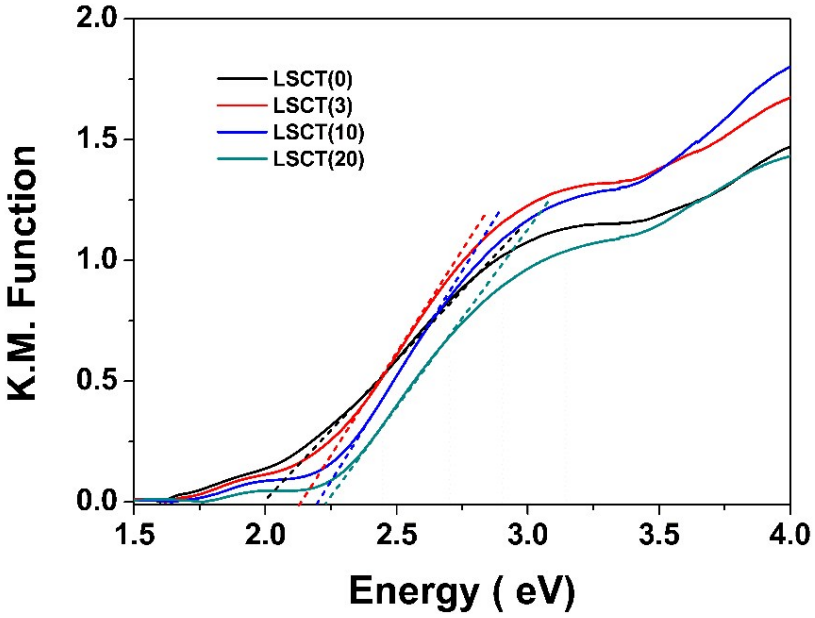

Fig. S8 Tauc plots of UV-vis absorbance spectra of LSCT samples.

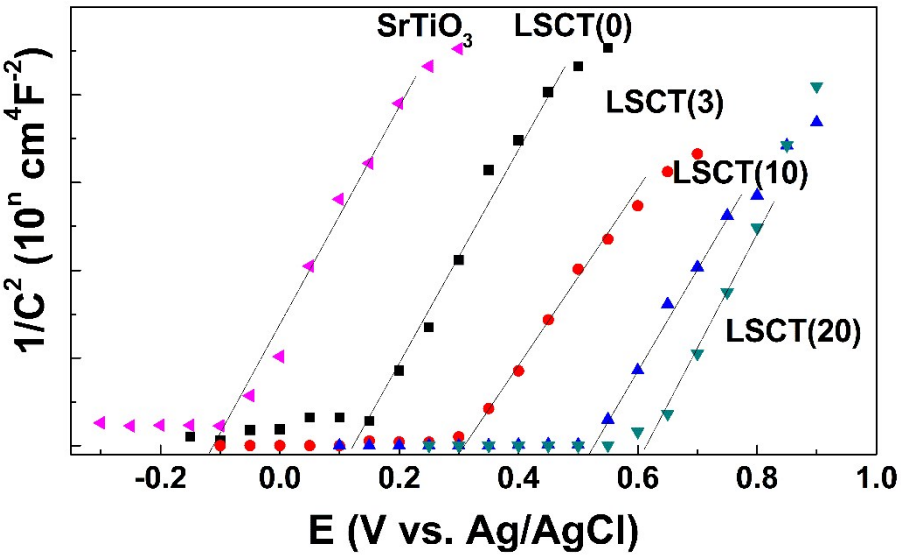

Fig. S9 Mott-Schottky measurements of LSCT samples along with $SrTiO_3$ for comparison.

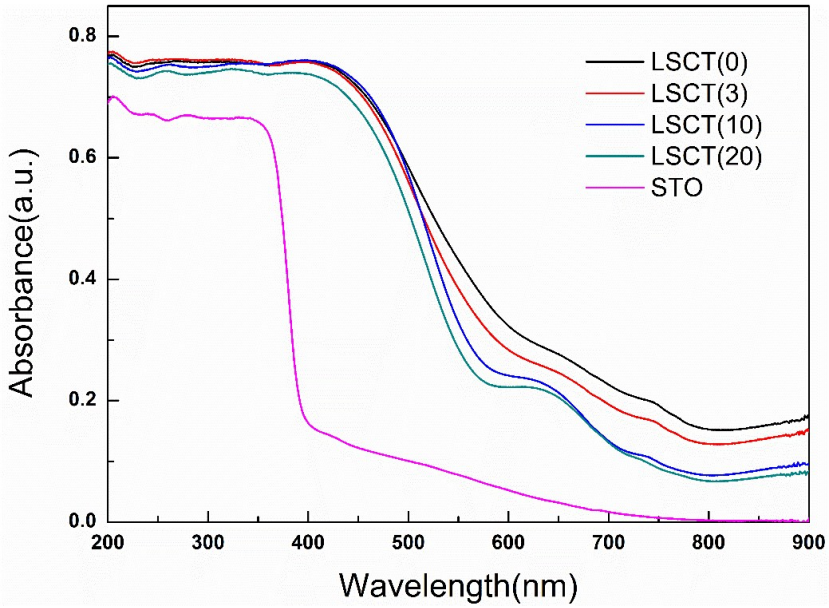

Fig. S10 UV-Vis absorbance spectra of LSCT pellet samples (without initial autozero).

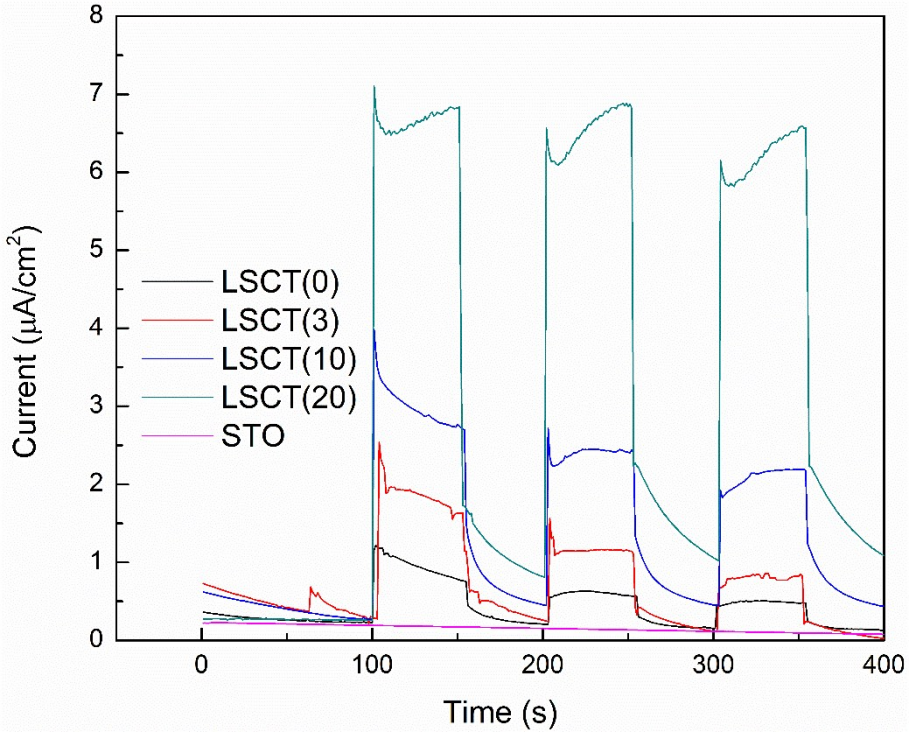

Fig. S11 Photocurrent response of LSCT samples under visible light (λ>420 nm) with potential bias of +0.4 V vs. Ag/AgCl in 5 M NaOH.

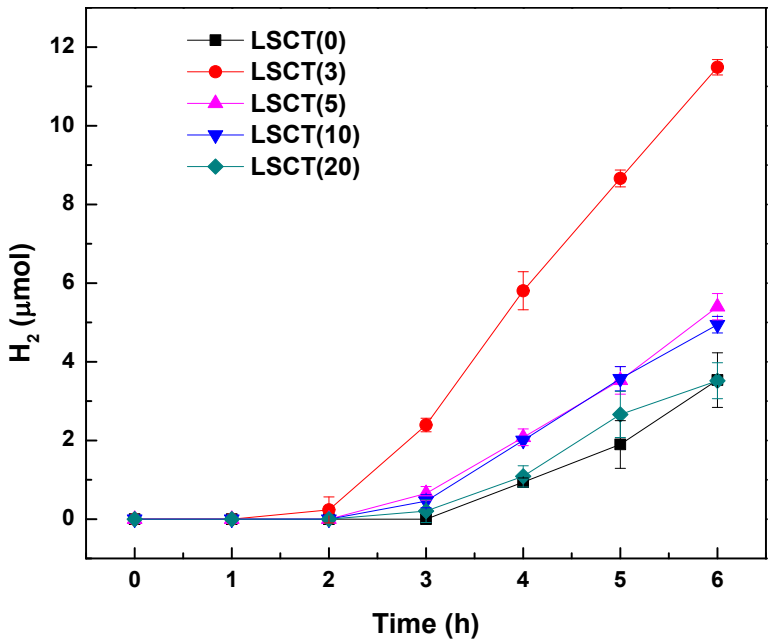

Fig. S12 Photocatalytic H_2 production with LSCT samples. Experimental condition: 100 mg LSCT powder suspended in 100 ml 5 M NaOH solution filled with 10 vol. % methanol. Visible light irradiation (≥ 420 nm) was given from an iron-doped halide lamp. Ar gas purging of sealed photo reactor for 0.5 h before irradiation.